Surface & Coatings Technology 258 (2014) 531–538

Contents lists available at ScienceDirect

Surface & Coatings Technology

journal homepage: www.elsevier.com/locate/surfcoat

Synthesis of porous ZnO/TiO_2 thin films with superhydrophilicity and photocatalytic activity via a template-free sol–gel method

Yanfeng Chen, Chaojie Zhang, Weixin Huang, Chunxiao Yang, Tao Huang, Yue Situ *, Hong Huang *

School of Chemistry and Chemical Engineering, South China University of Technology, Guangzhou 510640, PR China

ARTICLE INFO

Article history:
Received 7 May 2014
Accepted in revised form 19 August 2014
Available online 24 August 2014

Keywords:
Superhydrophilic
ZnO/TiO_2 thin film
Porous structure
Surface hydroxyl
Photocatalytic performance
Phase separation

ABSTRACT

Superhydrophilicity of TiO_2 thin film under natural conditions is of great importance for antifogging and self-cleaning applications of glass products. Transparent superhydrophilic porous ZnO/TiO_2 composite films were prepared on glass substrates using a template-free sol–gel method. The results indicated that the porous ZnO (10%)/TiO_2 composite film possesses superhydrophilicity with water contact angle less than 5° without UV irradiation. Surface chemical composition of the films was characterized by X-ray photoelectron spectroscopy (XPS). The morphologies of the porous films were characterized by scanning electron microscopy (SEM) and atomic force microscopy (AFM). The porous morphology, crystal structure and surface chemical composition were significantly affected by ZnO addition. The natural superhydrophilic performance was attributed to the synergistic effect of the porous structure and surface hydroxyl groups. Photocatalytic activities of the ZnO/TiO_2 composites were also evaluated using methyl orange (MO) as a model pollutant, with 78.1% of MO degraded by ZnO (10%)/TiO_2, which was higher than 49.3% obtained from pure TiO_2.

1. Introduction

Many efforts have been dedicated to the development of TiO_2 superhydrophilic films (water contact angle less than 5°) due to its great industrial applications like self-cleaning, antifogging, fluid drag reduction and bacteria-resistant [1–5]. TiO_2 film, unfortunately, tends to lose its superhydrophilicity within minutes to hours without ultraviolet (UV) illumination and this thus limits its application [6–8]. Appropriate chemical modifications such as ion doping [9], metal deposition [10,11] and semiconductor coupling [12] could make TiO_2 thin film approach superhydrophilicity under natural conditions. Zinc oxide, which is one of the important semiconductors, is often selected as a doped material due to its advantages of cheap, non-toxic, optical and photochemical properties [13–15]. The introduction of ZnO to TiO_2 film could improve the optical absorption property, an increased surface area and a more efficient separation of photogenerated electron–hole pairs which lead to the enhancing of photocatalytic activity [16,17]. Furthermore, surface wetting behavior was influenced by surface chemical composition. To the best of our knowledge, few studies concern the effect of ZnO on the surface chemical composition and the hydrophilicity of TiO_2 films.

Sol–gel method is one of the most widely used techniques for fabrication of TiO_2 films [18–20]. Especially, sol–gel processes are quite effective in producing multicomponent oxide films and also tuning film surface structure. Previous studies conducted by Wenzel [21] and Cassie-Baxter [22] suggested that improving surface roughness with hierarchical or porous structures can enhance the hydrophilicity of TiO_2 films. It was also reported that the multifunctional nanoporous thin films can facilitate the rapid infiltration of water into 3-D nanoporous network and thus enhance surface hydrophilicity [23]. Several templates including polyethylene glycol (PEG) [24–26], sodium dodecylbenzenesulfonate (DBS) [27], Pluronic (P123) block copolymer [28] and Pluronic F127 [29,30] have been successfully used for fabricating porous hydrophilic TiO_2 films via the sol–gel method. In our previous study, superhydrophilic porous TiO_2 film was prepared using a template-free sol–gel method in the presence of stabilizing agents (diethanolamine (DEA) and acetylacetone (AcAc)) [31–34]. A promising means is proposed to prepare natural superhydrophilic thin film by taking advantage of its combination of porous structure and the composition of ZnO/TiO_2.

In this study, the ZnO/TiO_2 thin films were prepared by intensively mixing the phase-separation-derived TiO_2 sol with ZnO sol before spin-coating and characterized by scanning electron microscopy (SEM), atomic force microscope (AFM) and X-ray diffraction (XRD).

* Corresponding authors. Tel./fax: +86 20 87112093.
E-mail addresses: situyue@scut.edu.cn (Y. Situ), cehhuang@scut.edu.cn (H. Huang).

http://dx.doi.org/10.1016/j.surfcoat.2014.08.042
0257-8972/

Furthermore, the properties of the composition films, such as self-cleaning, optical and photocatalytic abilities, are also significant for their applications. Superhydrophilicity, transparency, chemical composition and photocatalytic properties of the ZnO/TiO_2 films were also examined.

2. Materials and methods

2.1. Materials

Zinc acetate (Zn $(CH_3COO)_2 \cdot 2H_2O$, 99.0%) was obtained from Guangzhou Chemical Reagent Co., China. Anhydrous ethanol (C_2H_5OH, 99.7%), diethanolamine (NH $(CH_2CH_2OH)_2$; DEA, 99.0%), tetrabutyl titanate (Ti $(OC_4H_9)_4$, 98.5%), and acetylacetone ($CH_3COCH_2COCH_3$, AcAc, 98%) were purchased from Jiangsu Yonghua Fine Chemicals Co., China. Concentrated nitric acid (HNO_3, 66–68%) was obtained from Guangdong Guanghua Chemicals Co., China. Commercial P25 TiO_2 (Degussa) with an anatase/rutile ratio of 80/20 was used as the reference photocatalyst.

2.2. Preparations of precursor sols

The preparation of ZnO sol was conducted by dissolving 7.6 g of zinc acetate (Zn $(CH_3COO)_2 \cdot 2H_2O$, 99.0%) in anhydrous ethanol (C_2H_5OH, 99.7%), followed by the addition of diethanolamine (NH $(CH_2CH_2OH)_2$; DEA, 99.0%). The mixture solution was allowed to stir for 2 h at 60 °C. The relative molar ratio of each component in the precursor sol was Zn $(CH_3COO)_2$:C_2H_5OH:DEA: H_2O = 1:20:1:2. Moreover, the ZnO sol was aged for 24 h before mixing with TiO_2 sol. The TiO_2 sol was prepared by means of template-free sol–gel method based on our previous studies [31,34]. A homogeneous yellow solution was obtained by mixing 10 mL tetrabutyl titanate (Ti $(OC_4H_9)_4$, 98.5%) with 40 mL of anhydrous ethanol. Then acetylacetone ($CH_3COCH_2COCH_3$, AcAc, 98%) and diethanolamine ($(HOCH_2CH_2)_2NH$, DEA, 99%) were added in order. After stirring for 30 min, the mixture of 20 mL ethanol, 10 mL deionized water and 1 mL HNO_3 solution (66–68% mass fraction) was dropped in and the stirring continued for 3 h at room temperature. The relative molar ratio of each component in the precursor sol was Ti $(OC_4H_9)_4$:C_2H_5OH:AcAc:DEA:H_2O:HNO_3 = 1:35:0.65:0.7:20:0.5.

2.3. Preparation of porous ZnO/TiO_2 composite films

Different ZnO/TiO_2 composite sols varying in the content of ZnO in the composite were obtained by adding different volumes of ZnO sol into a certain amount of TiO_2 sol. We can obtain the desired ZnO/TiO_2 composite sols containing a mole fraction of 10%, 20%, 30% and 40%, which were used for composite film preparation. Composite sols were stirred for 2 h and aged at room temperature for 2 days before spin coating.

Glass substrates were washed successively with acetone, anhydrous ethanol and deionized water in an ultrasound bath. Dried glass substrates were spin-coated by the composite sols with rotation speed of 800 rpm for 20 s and 3000 rpm for 30 s. The experiment was repeated 3 times to obtain the desired thickness of the films. The final coatings were dried at 110 °C for 30 min and then calcined in air at 500 °C for 30 min, at a heating rate of 5 °C/min. The pure TiO_2 and the as-prepared ZnO/TiO_2 composite powders were obtained by drying and annealing the gels. Finally, the powders were collected for XRD characterization and photocatalytic measurement. The as-prepared film samples were used for other characterizations.

2.4. Surface wettability measurements

The superhydrophilicity of the films was evaluated by water contact angle measurements with a JC2000C1 contact angle goniometer from Shanghai POWEREACH Co. China. Advancing and receding contact angles were recorded by a camera with 500 frames per second, namely time interval of adjacent photo is 2 ms. Each reported value of contact angle is the average of five measurements made at different places on the film surface. Sample for antifogging behavior test was prepared by the washed glass substrate (2.5 cm × 7.5 cm) and half of the glass substrate was coated with the ZnO (10%)/TiO_2 composite film at the same condition. Boiling water was added into a beaker. The sample was placed on the beaker with coated surface facing down for 5 min. Vapor condensed on the coating surface was observed and photographed. Three ZnO (10%)/TiO_2 films were additionally prepared to test the stability of wetting behavior. Then the ZnO (10%)/TiO_2 films were kept at three different conditions: i) dark, the noncovered sample was simply left on the benchtop in a dark box; ii) laboratory conditions, the noncovered sample was simply left on the benchtop; iii) vacuum condition, the sample was placed in a vacuum oven at room temperature. Water contact angles for the samples were measured with a time interval of three days.

2.5. Photocatalytic measurements

The photocatalytic activities of the pure TiO_2, P25 and the as-prepared ZnO/TiO_2 composite powders were evaluated by degrading methyl orange (10.3 mg L^{-1}) in H_2O. First, 40 mg of the powder photocatalyst was combined with the 40 mL of the dye solution in a 50 mL quartz round-bottom flask and was stirred for 30 min to reach the adsorption–desorption equilibrium in a dark box. The suspension was transferred to a water-cooled reactor and irradiated under a solar simulator with an AM1.5 filter (Perfect Light XPS 700 Xe lamp, Beijing Perfectlight Technology Co., Ltd, 100 mW cm^{-2} illumination intensity). Four milliliter aliquot was withdrawn at certain time intervals and then centrifuged (5000 rpm, 10 min) to remove the particles. The absorbance at 462 nm (methyl orange absorbance maximum) was recorded by a Shimadzu UV-2050 spectrophotometer.

2.6. Characterizations

The surface morphologies of the TiO_2 film and the as-prepared ZnO/TiO_2 composite films with varying ZnO content were observed by an S-3700N scanning electron microscopy (SEM). Cross-section view of ZnO (10%)/TiO_2 film was observed by a ZEISS field-emission scanning electron microscopy (FE-SEM). Atomic force microscopy (AFM) measurement was performed using an instrument (CSPM 2003) with 3 μm × 3 μm scanned area and images were acquired under ambient conditions in contact mode using a Nanoprobe cantilever. The powder X-ray diffraction (XRD) patterns of the prepared powder were recorded on a Bruker D8 ADVANCE X-ray diffractometer with Cu Ka radiation (1.54178 Å). UV–vis diffuse reflectance spectra of the films were recorded in a Hitachi Corporation UV-3010 spectrophotometer. Surface chemical compositions of the as-prepared films were analyzed by a VG Scientific ESCA LAB MK II X-ray photoelectron spectroscopic (XPS). The XPS data was analyzed using the XPSPeak 4.1 program [35,36].

3. Results and discussion

3.1. Morphology of porous ZnO/TiO_2 composite thin films

As shown in Fig. 1a, the porous TiO_2 film exhibits numerous macropores with a size around 3.0 μm. Fig. 1b–e shows SEM images of porous ZnO/TiO_2 composite films prepared by introducing different amounts of ZnO sol into TiO_2 sol to reach a ZnO molar content of 10, 20, 30 and 40% in the ZnO/TiO_2 composite films. The morphology especially pore size significantly depends on the ZnO content. As the molar content of ZnO was 10% (Fig. 1b), the pore size (approximately 6.0 μm) of ZnO/TiO_2 composite films becomes larger, compared to that of pure TiO_2 films. Meanwhile, a certain amount of smaller pores at

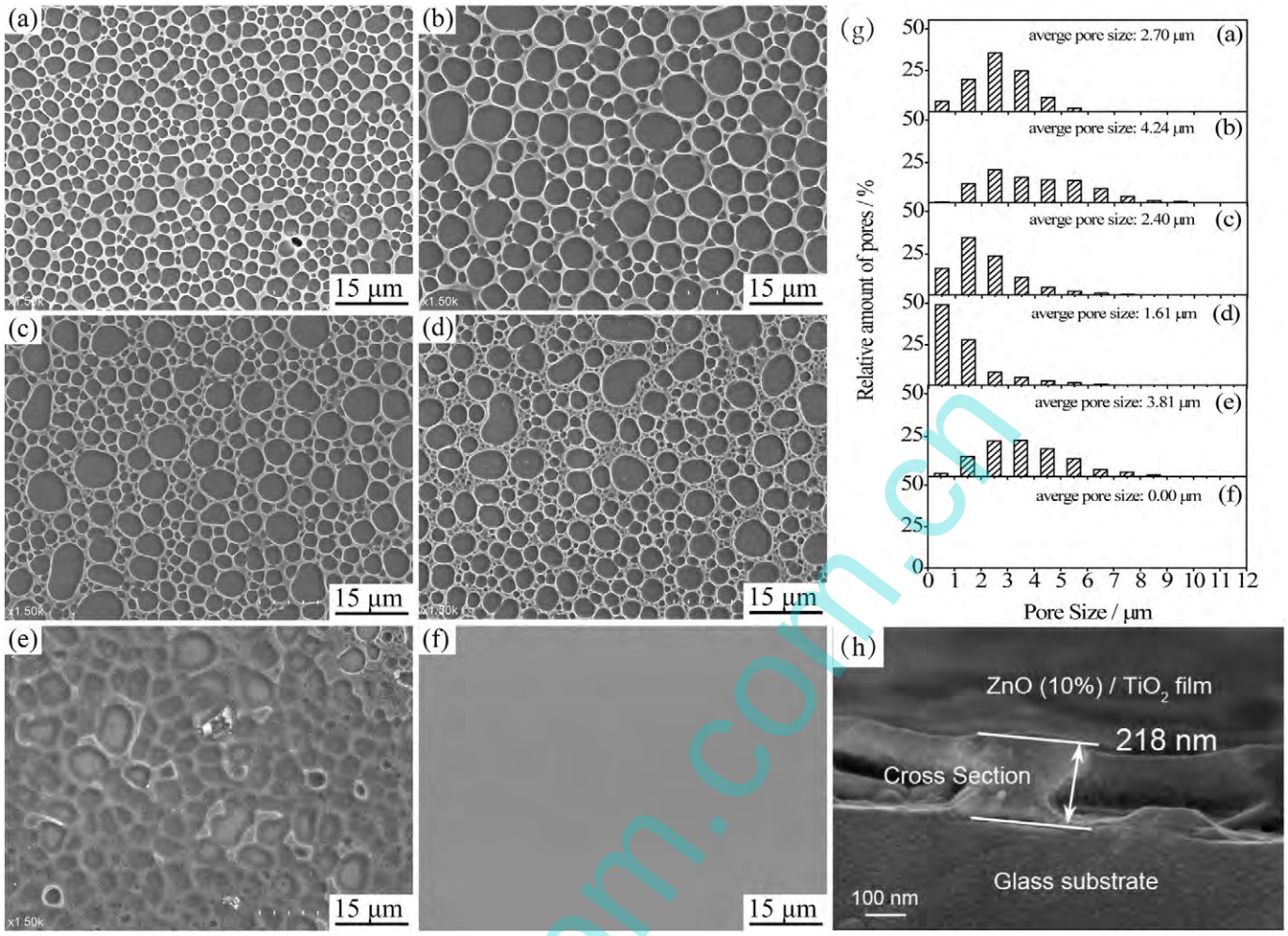

Fig. 1. SEM images of pure porous TiO_2 thin film (a), as-prepared porous ZnO (10, 20, 30 and 40%)/TiO_2 composite thin films (b)–(e), pure flat ZnO film (f), a statistical distribution of pore sizes (g) and cross-section image of ZnO (10%)/TiO_2 film (h).

around 2.0 μm appears among the larger pores. When the ZnO molar fraction is increased to 20% (Fig. 1c), two significant population (larger and smaller pores) co-existing on the surface can be observed. The size of smaller pores is about 1.5 μm and the number of larger pores becomes smaller at the same time. Fig. 1d illustrates that pore size became different with larger pores (approximately 8.0 μm) and smaller pores (less than 1.0 μm) in the films containing 30% ZnO. However, when the amount increases to 40% (Fig. 1e), bicontinuous pore structure turns to be less defined. The pore depth of ZnO (40%)/TiO_2 film becomes shallow, but porosity of the film remains. From upper right of Fig. 1e, size of small pores turns to be much smaller (nano-pores). Fig. 1f shows a flat ZnO film without porous structure. A statistical distribution of pore sizes for the samples is presented in Fig. 1g. The average pore sizes of pure TiO_2 and ZnO (10, 20, 30 and 40%)/TiO_2 films are 2.70, 4.24, 2.40, 1.61 and 3.81 μm. The SEM image of a cross-section (Fig. 1h) of the ZnO (10%)/TiO_2 film indicates clearly that the film has porous structure. The as-prepared ZnO (10%)/TiO_2 film has a thickness of about 218 nm and the pore depth is about 200 nm. Actually, ZnO/TiO_2 films with a three-dimensional porous structure were finally obtained. AFM images of ZnO (10%)/TiO_2 film, as shown in Fig. 2, display that the parameters (porous structure and pore depth) are close to those shown in the cross-sectional view. It appears, then, that the formation of pores taking place in the TiO_2 sol was suppressed gradually by the addition of ZnO sol. However, the given results are inspiring us that porous structures of ZnO/TiO_2 films still remained in a large range addition of ZnO sol (from 10% to 30%), which undoubtedly attain the synergistic properties of porous structure and composite materials.

Our previous works have found that porous TiO_2 films can be prepared by the template-free sol–gel method utilizing two complexing agents including AcAc and DEA ($Ti(OBu)_{4-x}(AcAc)_x$ or $Ti(OBu)_{4-x}(DEA)_x$), as shown in Scheme 1, where the rate of hydrolysis and polycondensation of the metal alkoxides was controlled effectively [31,34]. When 10% ZnO was introduced into TiO_2 sol, the pH of ZnO/TiO_2 sol was 6.64 that enhanced significantly compared to pure TiO_2 sol. With the increase amount of ZnO to TiO_2 sol, the start pHs of ZnO/TiO_2 composite sols (10, 20, 30 and 40%) were 6.64, 6.58, 6.56 and 6.53, respectively (Table 1). There is no obvious pH difference in the ZnO/TiO_2 sol system owing to the co-existing of weak-acid (CH_3COO^-) and weak-base (DEA^+) salt. Therefore, when ZnO sol with non-phase-separation is introduced to the TiO_2 sol system which means polar (solvent in ZnO sol) and nonpolar (ZnO oligomers in ZnO sol) solvents are added into both polar phase and nonpolar phase of the original TiO_2 sol system. The domains of phase separation of TiO_2 sol are diluted, and polarity differences between polar phase and nonpolar phase decrease as well. With the increase of the amount of ZnO sol (10, 20, 30 and 40%), polarity differences of both phases decrease. Usually, a phase with minor volume fraction will be dispersed within the major continuous phase if the highly polarity differs on both phases [37]. On this occasion, minor solvent phase has a tendency to combine with other minor solvent phase to develop a large solvent domain resulting in the large pores in the process of drying. On the contrary, the decrease of polarity differences poses an obstacle to the

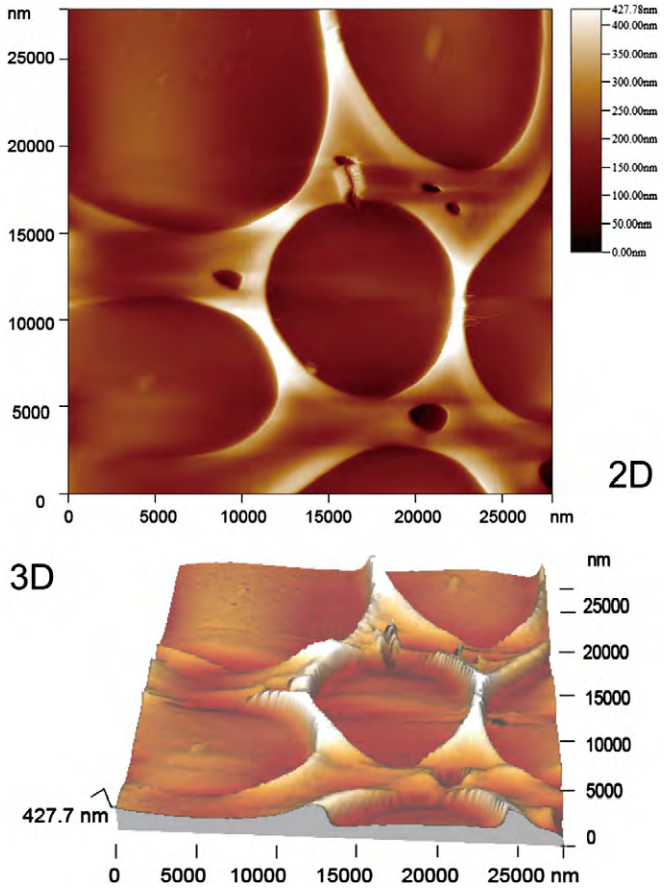

Fig. 2. Atomic force microscope images (2D and 3D) of ZnO (10%)/TiO_2 film.

combination of the minor solvent phases and thus the large amounts of small pores are formed.

3.2. X-ray diffraction studies

The crystal structures of the corresponding pure TiO_2, pure ZnO and as-prepared ZnO/TiO_2 composite samples were measured by XRD characterization. XRD pattern of pure TiO_2 sample (Fig. 3a) reveals the typical peaks at around $2\theta = 25.3$, 37.8, 47.9, 53.8, 55.1, 62.7, 68.7, 70.3 and 75.0°, which are attributed to the (101), (004), (200), (105), (211), (204), (116), (220) and (215) planes. These peaks confirm

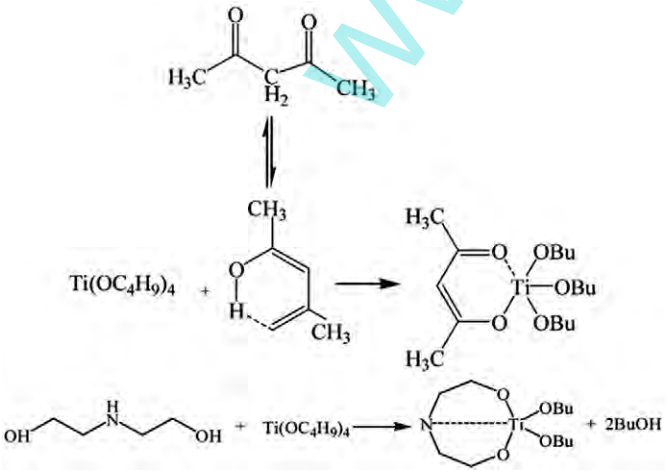

Scheme 1. A suggest formation mechanism of $Ti(OC_4H_9)_4$ chelating with AcAc and DEA.

Table 1
pH of pure TiO_2 and as-prepared ZnO/TiO_2 composite sols.

Sample	TiO_2	ZnO	10%	20%	30%	40%
pH	6.18	7.13	6.64	6.58	6.56	6.53

the presence of polycrystalline anatase structure in the TiO_2 sample [38,39]. The pure TiO_2 sample has anatase (101) plane peaks but no rutile (100) plane peaks, indicating that only the anatase crystalline phase is present. As revealed in Fig. 3f, the typical diffraction peaks at around $2\theta = 31.8$, 34.6, 36.3, 47.7, 56.7, 62.9, 66.6, 68.1, 69.2, 72.6 and 77.0°, are attributed to the (100), (002), (101), (102), (110), (103), (200), (112), (201), (004) and (202) crystal planes, respectively. All the diffraction peaks of the ZnO sample can be demonstrated with the existence of wurtzite ZnO crystal structure [40]. With the increasing content of ZnO (from 10 to 20% molar fraction), the characteristic peaks of anatase TiO_2 gradually decrease, which was shown in Fig. 3b–c. It should be noted that even at the ZnO content of 20% molar fraction, no obvious diffraction peak assigned to the crystal phase of the ZnO could be seen and this results suggest that some Zn^{2+} cations were incorporated into the titania network [41]. However, in the case of the larger content of ZnO in the ZnO/TiO_2 (from 30 to 40% molar fraction) composite samples, the peaks of anatase TiO_2 fade away (Fig. 3d–e). Alternatively, a broader peak at around $2\theta = 34.0°$ appears, which is probably ascribed to the wurtzite phase of ZnO [42]. The low intensities of the observed peaks in these cases suggested that the composite samples were rather amorphous. It was supposed that excess small nanoparticles of ZnO during the ZnO/TiO_2 sol preparation did not favor the crystallizing process during the heating procedure, leading to a poor crystallization behavior for the composite sample [43].

3.3. Optical transmittance of ZnO/TiO_2 composite films

From a technical point of view of antifogging and self-cleaning applications, transmittance of TiO_2 films is of great importance to be considered. The pure TiO_2, pure ZnO and ZnO (10, 20, 30 and 40%)/TiO_2 composite films were spin-coated three times at the same condition to eliminate the thickness difference. The transmission spectra of pure TiO_2, pure ZnO and as-prepared ZnO/TiO_2 composite films were displayed in Fig. 4. The average optical transmission of pure TiO_2 film in the visible range part of the spectrum is found to be about 91%, which is attributed to high refraction coefficient of TiO_2 thin films. Surface morphology has a significant effect on the optical properties of the film. Larger pores result in the reduction of light scattering, which can improve the transmittance of porous film [44]. For ZnO (10 and 20%)/TiO_2 films, a slight rise in transmittance is observed

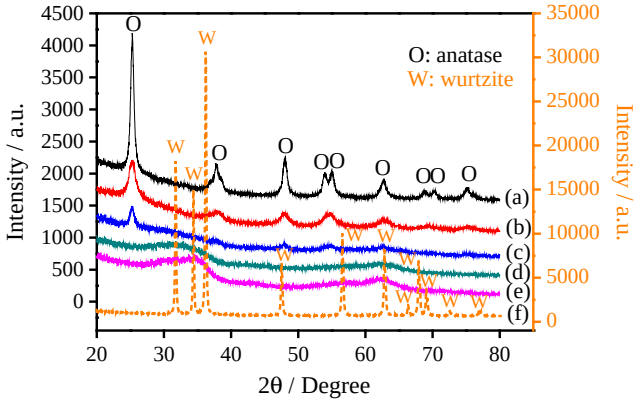

Fig. 3. XRD patterns of the corresponding powder samples of pure TiO_2 (a), ZnO (10, 20, 30 and 40%)/TiO_2 composite (b–e) and pure ZnO (f).

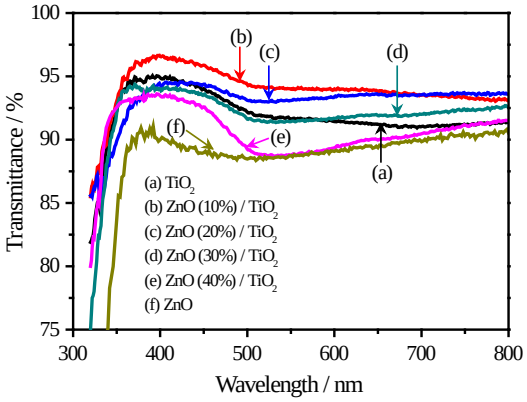

Fig. 4. Transmittance spectra of pure TiO_2 film (a), ZnO (10, 20, 30 and 40%)/TiO_2 film (b–e), and ZnO film (f).

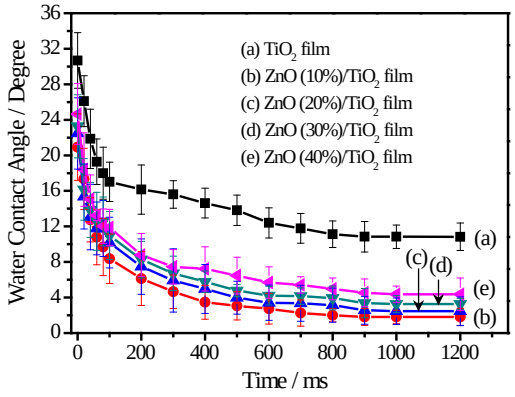

Fig. 6. Time-dependent changes in instant water contact angle as a function of pure TiO_2 film (a), and ZnO (10, 20, 30 and 40%)/TiO_2 film (b–e).

(Fig. 4b–c). The phenomenon can be explained that larger pores of ZnO (10 and 20%)/TiO_2 films hold dominant position in the transmittance of the films. With increasing ZnO molar content (up to 40%), different variation of optical transmittance in the visible range can be observed: a decrease in 500–800 nm range and an increase in the 400–500 nm range (Fig. 4e). The decrease in transmittance at about 500 nm may be due to increasing optical scatting caused by increasing grain boundary density in the more rough, uneven and porous ZnO (40%)/TiO_2 film. Pure ZnO film has the same trend in the transmission as ZnO (40%)/TiO_2 film, which was similar with the result reported before [44].

3.4. Superhydrophilicity of porous ZnO/TiO_2 composite thin films

Superhydrophilic surfaces have considerably practical applications for self-cleaning and antifogging thanks to their special properties [4,23]. Still images obtained from the camera image data show that a first drop of water wets the surfaces of pure TiO_2 film and ZnO (10%)/TiO_2 film in about 800 ms (Fig. 5). Compared to that of pure TiO_2 film, the water drop was almost completely spread out on the ZnO (10%)/TiO_2 film. Time-dependent changes in instant water contact angle were also studied. As shown in Fig. 6a, pure TiO_2 film shows that hydrophilicity with water contact angle (WCA) was relatively large (10.8°) and water droplet spreads on the surface within 800 ms. Precious studies have shown the flat TiO_2 film has hydrophilicity with a water contact angle of 20.5° and 15° in the works of Huang and Yu, respectively [32,45]. The result indicates that the porous surface has strongly improved the hydrophilicity of TiO_2 film. With the addition of ZnO, porous ZnO (10, 20 and 30%)/TiO_2 composite films show superhydrophilicity even without UV light irradiation and WCAs of ZnO/TiO_2 composite films turn into 1.8, 2.5 and 3.2°, respectively (Fig. 6b–d). There is a large difference in surface morphology between ZnO (40%)/TiO_2 film and ZnO (10, 20 and 30%)/TiO_2 film (Fig. 1), which the pore depth of ZnO (40%)/TiO_2 film becomes shallow. However, the porosity of ZnO (40%)/TiO_2 film remains. A statistical distribution of pore sizes shows that ZnO (40%)/TiO_2 film has similar pore distribution to that of ZnO (10%)/TiO_2 film (Fig. 1g). Therefore, it is reasonable that ZnO (40%)/TiO_2 film has water contact angle of 4.4°, which is a little different from those of ZnO (10, 20 and 30%)/TiO_2 film. These features suggest that the addition of ZnO in ZnO (10, 20, 30 and 40%)/TiO_2 composite films reveals the additive effect on superhydrophilicity.

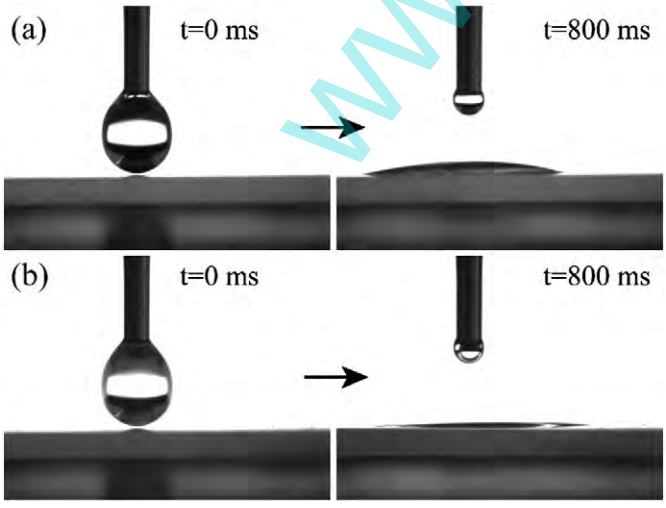

Fig. 5. Still images from the camera contact angle measurements for a first drop of water of pure TiO_2 film (a) and ZnO (10%)/TiO_2 film (b).

3.5. Study of superhydrophilicity mechanism of porous ZnO/TiO_2 composite thin films

Hydroxyl groups on the surface of films significantly promoting hydrophilic of TiO_2 film have been widely accepted [46]. In order to determine surface chemical composition and the ability of absorbing hydroxyl groups, pure TiO_2 film and ZnO (10%)/TiO_2 film were studied by XPS analysis. Table 2 showed the atomic concentration fraction of the as-prepared films. Sodium (Na) and silicon (Si) elements were found, which came from the diffusion from substrate to film during calcination. The actual composition and atomic concentration of Ti and Zn for the two samples analyzed by XPS are a certain amount of difference from nominal values that may be due to characterization difference on regional position of the films. The XPS survey spectrum of the as-prepared films was shown in Fig. 7. The peak positions in all of the XPS spectra were calibrated with C 1s at 284.6 eV. The O 1s, Ti 2p, C 1s, Si 2s and Si 2p could be easily observed in the survey spectrum of pure TiO_2 film. With the addition of ZnO, Zn 2p appears in the survey spectrum of ZnO (10%)/TiO_2 film. The binding energies (BE) of various peaks obtained from fitting procedures were listed in Table 3 for pure TiO_2 film and ZnO (10%)/TiO_2 film. The O 1s high-resolution spectrum in Fig. 8 can be fitted into four peaks for pure TiO_2 film and five peaks for ZnO (10%)/TiO_2 film. The information about background type, peak position and full width at half maximum (FWHM) was listed in Table 3. The peak positions at 529.6, 531.1, 532.0, 532.6 and 530.6 eV

Table 2
Atomic concentration fraction (%).

Sample	Na 1s	O 1s	Ti 2p	Zn 2p	C 1s	Si 2p
Pure TiO_2	11.80	53.46	6.60	–	16.01	12.13
ZnO (10%)/TiO_2	11.40	52.27	3.81	1.49	18.37	12.65

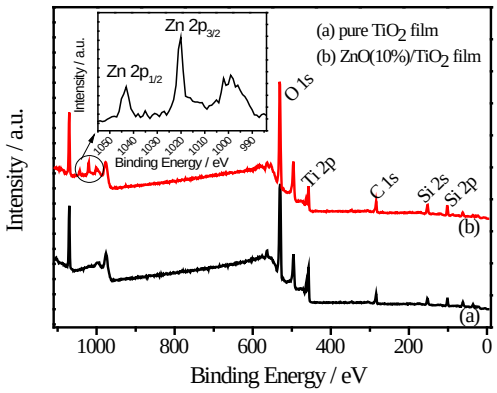

Fig. 7. XPS patterns of pure TiO_2 film (a) and as-prepared ZnO (10%)/TiO_2 composite film (b).

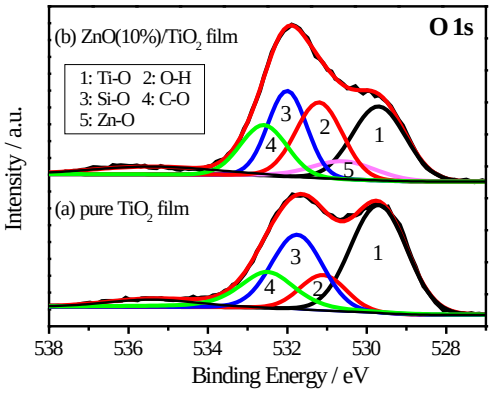

Fig. 8. High-resolution XPS pattern of O 1s for pure TiO_2 film (a) and as-prepared ZnO (10%)/TiO_2 composite film (b).

were ascribed to Ti – O, O – H, Si – O, C – O and Zn – O bond, respectively. The contents of the hydroxyl group in pure TiO_2 film surface and ZnO (10%)/TiO_2 film surface are 11.3% and 23.2%. The result suggests that the addition of ZnO in ZnO/TiO_2 composite film apparently enhances the amount of chemisorption of H_2O, which is reacting with TiO_2 to form Ti – OH [47], therefore increasing the surface hydroxyl groups. Previous research has shown that many binary metal oxides exhibited high surface acidity, for example, Tanabe et al. proposed that the surface acidity was attributed to M – O – M′ heterolinkages due to the charge imbalance and an excess of positive (Lewis sites) or negative (Bronsted sites) charge in the structure of binary metal oxides generated the acidity [48].

However, the superhydrophilicity of ZnO/TiO_2 films is not completely ascribed to the increasing adsorbed hydroxyl groups, the porous structure of the films also plays an important role in superhydrophilicity of the films without UV irradiation and this phenomenon could be attributed to two wetting regimes, either the Wenzel or the Cassie regime [21,22]. The Wenzel regime held the view that the increasing roughness of a surface could enhance its hydrophilicity in the case of a given hydrophilic chemical composition. While the Wenzel regime described wetting mechanism by the equation: $\cos\theta_w = r\cos\theta_0$, where θ_w and θ_0 were Wenzel contact angle and the Young's CA of a flat surface, and r was the roughness factor, defined as the total surface area to the projected area in the horizontal plane [25]. Cassie impregnating wetting regime, supposed that the mixed surface was composed of the solid and the test liquid, which describes heterogeneous wetting by the equation: $\cos\theta_c = 1 - \Phi s + \Phi s\cos\theta_0$, where θ_c and θ_0 were the Cassie contact angle and the Young's contact angle, respectively and Φs was the fraction of dry solid "island" in the mixed surface beyond the drop [25]. Thus, the wetting behavior results from porosity-driven superhydrophilicity partly. So, both surface hydroxyl groups and porous structure prepared by phase separation are attributed to the superhydrophilicity of ZnO/TiO_2 composite films.

3.6. Antifogging behavior and stability test of ZnO (10%)/TiO_2 film

The ZnO/TiO_2 composite film exhibits good superhydrophilicity which doubtlessly meets the requirement of antifogging. The antifogging behavior of superhydrophilic ZnO (10%)/TiO_2 composite film was studied. As could be seen in Fig. 9, the normal glass fogs soon (left side), and coated glass remains clear (right side). The condensed water droplet spread faster on the superhydrophilic surface and formed a thin sheet-like water membrane, thus keeping the coated glass a long time clear.

For testing the stability of the as-prepared superhydrophilic ZnO (10%)/TiO_2 film, the additional experiments about WCA versus time at different storage conditions have been carried out. As shown in Fig. 10, when superhydrophilic ZnO (10%)/TiO_2 film was simply stored in the dark, it required approximately 21 days for water contact angle to increase to 9.5°. When the film was placed in laboratory conditions, water contact angle was increased to 17.3°. It was likely caused by a recontamination of the surface by airborne hydrophobic organics [49,50]. However, when the film was stored in vacuum condition, water contact angle was increased to 30.2° because a dehydroxylation/dehydration process on the surface of ZnO (10%)/TiO_2 film took place when the film was stored in a vacuum oven [49].

3.7. Photocatalytic performance

Fig. 11 displays the photodegradation of MO as a function of irradiation time over pure TiO_2, P25 (as a reference photocatalyst) and ZnO (10, 20, 30 and 40%)/TiO_2 composites. Based on a blank experiment without any catalyst, the self-photolysis of MO under solar simulator irradiation could be ignored. It could be seen from Fig. 11 that 49.3, 78.1, 60.2, 7.5 and 8.7% of MO had been degraded over pure TiO_2 and ZnO (10, 20, 30 and 40%)/TiO_2 for 280 min, respectively. ZnO (10%)/TiO_2

Table 3
XPS fitting data of different samples.

Sample	Ti 2p	Zn 2p	Si 2s	Si 2p	O 1s	O 1s fitting			
	eV					Background type	Position (eV)	FWHM (eV)	Assignment
(a)	457.0	–	152.0	102.1	531.1	Shirley	529.6	1.65	Ti – O
							531.1	1.36	O – H
							532.0	1.51	Si – O
							532.6	1.63	C – O
(b)	457.0	1020.1	152.0	102.1	531.1	Shirley	529.6	1.58	Ti – O
							531.1	1.38	O – H
							532.0	1.15	Si – O
							532.6	1.37	C – O
							530.6	1.90	Zn – O

(a) Pure TiO_2; (b) ZnO (10%)/TiO_2.

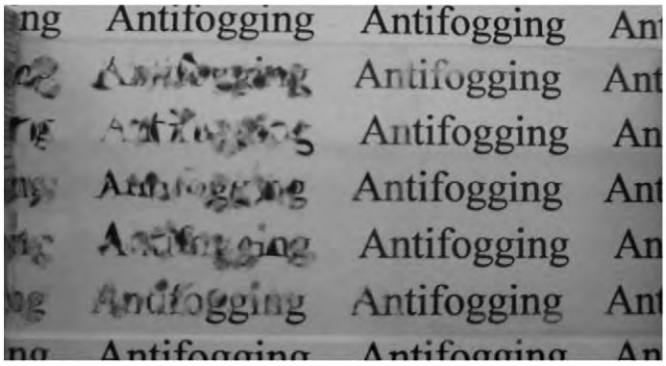

Fig. 9. Antifogging behavior of superhydrophilic porous ZnO (10%)/TiO_2 film, blank glass slide at left side and coated glass slide at right side.

exhibited the highest photocatalytic activity among the as-prepared samples, which increased degradation rate by 28.8% compared to the pure TiO_2. As the molar fraction of ZnO increased from 10 to 20%, a decrease in the photocatalytic activity of ZnO (20%)/TiO_2 was observed. The reason for this phenomenon is the suitable added amount of ZnO that can promote the separation of holes and electrons, which retain the maximum possible fraction of anatase TiO_2 that shows high photocatalytic activity [51]. With the 30 and 40% content of ZnO, inferior photocatalytic activity of ZnO (30%)/TiO_2 and ZnO (40%)/TiO_2 could be seen from Fig. 11d–e.

4. Conclusions

Phase separation derived porous ZnO/TiO_2 composite films were prepared via sol–gel method, and the porous composite films exhibited appreciable superhydrophilicity with water contact angles 1.8° only without UV irradiation. The porous structure was prepared with the polymerization-induced phase separation. The adding of ZnO sol weakens the polymerization in the system decreasing the tendency of phase separation. Superhydrophilicity mechanism of porous ZnO/TiO_2 composite thin films was further investigated, which showed that the wetting behavior resulted from porosity-driven superhydrophilicity partly. Both surface hydroxyl groups and porous structure prepared by phase separation are attributed to the superhydrophilicity of ZnO/TiO_2 composite films. The addition of ZnO in ZnO/TiO_2 composites also revealed the enhanced photocatalytic performance. ZnO (10%)/TiO_2 composites exhibited the enhanced photocatalytic performance with 78.1% MO degradation rate (comparing to TiO_2 of 49.3%). Therefore, the use of porous ZnO/TiO_2 composite films shows advantages of lower cost, better superhydrophilicity in natural condition and enhanced photocatalytic activity. These advantages enable them to be employed as a promising hydrophilic material for glass antifogging and self-cleaning applications.

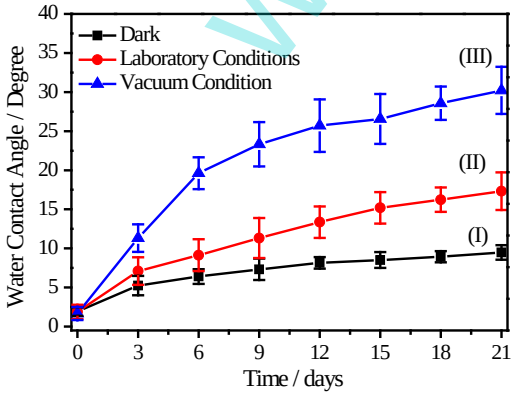

Fig. 10. Water contact angle versus time for ZnO (10%)/TiO_2 film at different conditions: dark (I), laboratory conditions (II) and vacuum condition (III).

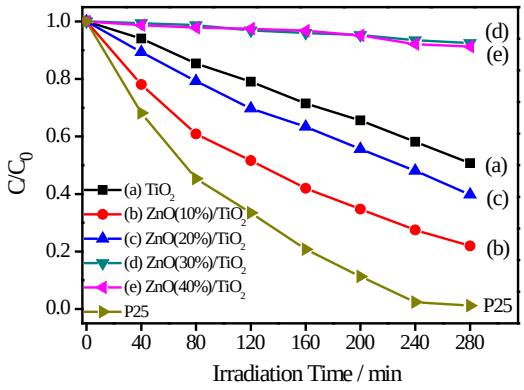

Fig. 11. Photocatalytic activities of pure TiO_2 and as-prepared ZnO/TiO_2 composites on the degradation of MO under solar simulator irradiation.

Acknowledgment

The authors gratefully thank the "National Natural Science Foundation of China (no. 51103045)" for financial support of this work. We are also grateful to Professor Dr. Chunhua Feng from the Key Lab of Pollution Control and Ecosystem Restoration in Industry Clusters, Ministry of Education School of Environment and Energy, South China University of Technology for polishing the language.

References

[1] Z. Wu, D. Lee, M.F. Rubner, R.E. Cohen, Small 3 (2007) 1445.
[2] Y. Lai, Y. Tang, J. Gong, D. Gong, L. Chi, C. Lin, Z. Chen, J. Mater. Chem. 22 (2012) 7420.
[3] S. Nishimoto, B. Bhushan, Rsc Adv. 3 (2013) 671.
[4] A. Tricoli, M. Righettoni, S.E. Pratsinis, Langmuir 25 (2009) 12578.
[5] D. Glöß, P. Frach, O. Zywitzki, T. Modes, S. Klinkenberg, C. Gottfried, Surf. Coat. Technol. 200 (2005) 967.
[6] A. Nakajima, S.i. Koizumi, T. Watanabe, K. Hashimoto, Langmuir 16 (2000) 7048.
[7] M. Miyauchi, A. Nakajima, A. Fujishima, K. Hashimoto, T. Watanabe, Chem. Mater. 12 (2000) 3.
[8] H.S. Lim, D. Kwak, D.Y. Lee, S.G. Lee, K. Cho, J. Am. Chem. Soc. 129 (2007) 4128.
[9] S.D. Sharma, D. Singh, K. Saini, C. Kant, V. Sharma, S. Jain, C. Sharma, Appl. Catal. A Gen. 314 (2006) 40.
[10] K. Sunada, T. Watanabe, K. Hashimoto, Environ. Sci. Technol. 37 (2003) 4785.
[11] Y. Liang, K. Lu, Int. J. Appl. Ceram. Technol. 9 (2011) 911.
[12] Y. Lai, Z. Lin, J. Huang, L. Sun, Z. Chen, C. Lin, New J. Chem. 34 (2010) 44.
[13] Z. Liu, Z. Jin, W. Li, J. Qiu, Mater. Lett. 59 (2005) 3620.
[14] T.S. Li, G. He, W.D. Li, B. Deng, M. Zhang, C.Y. Zheng, Z.Q. Sun, Sci. Adv. Mater. 6 (2014) 908.
[15] R. Fateh, R. Dillert, D.W. Bahnemann, ACS Appl. Mater. Interfaces 6 (2014) 2270.
[16] D. Chen, H. Zhang, S. Hu, J. Li, J. Phys. Chem. C 112 (2008) 117.
[17] L. William IV, I. Kostedt, A.A. Ismail, D.W. Mazyck, Ind. Eng. Chem. Res. 47 (2008) 1483.
[18] C.L. Liu, R.Y. Li, W.J. Zhang, Appl. Mech. Mater. 48 (2011) 153.
[19] J. Yu, X. Zhao, J. Du, W. Chen, J. Sol–Gel Sci. Technol. 17 (2000) 163.
[20] D. Macwan, P.N. Dave, S. Chaturvedi, J. Mater. Sci. 46 (2011) 3669.
[21] R.N. Wenzel, Ind. Eng. Chem. 28 (1936) 988.
[22] A. Cassie, Discuss. Faraday Soc. 3 (1948) 11.
[23] F.Ç. Cebeci, Z. Wu, L. Zhai, R.E. Cohen, M.F. Rubner, Langmuir 22 (2006) 2856.
[24] S. Bu, Z. Jin, X. Liu, L. Yang, Z. Cheng, J. Eur. Ceram. Soc. 25 (2005) 673.
[25] W. Huang, M. Lei, H. Huang, J. Chen, H. Chen, Surf. Coat. Technol. 204 (2010) 3954.
[26] S.H. Wang, K.H. Wang, Y.M. Dai, J.M. Jehng, Appl. Surf. Sci. 264 (2013) 470.
[27] Y. Qu, S. Song, L. Jing, Y. Luan, H. Fu, Thin Solid Films 518 (2010) 3177.
[28] H. Uchida, M.N. Patel, R.A. May, G. Gupta, K.J. Stevenson, K.P. Johnston, Thin Solid Films 518 (2010) 3169.
[29] J. Zita, J. Krýsa, U. Černigoj, U. Lavrenčič-Štangar, J. Jirkovský, J. Rathouský, Catal. Today 161 (2011) 29.
[30] S.R. Patil, B. Hameed, A.S. Škapin, U.L. Štangar, Chem. Eng. J. 174 (2011) 190.
[31] W. Huang, W. Deng, M. Lei, H. Huang, Appl. Surf. Sci. 257 (2011) 4774.
[32] T. Huang, W. Huang, C. Zhou, Y. Situ, H. Huang, Surf. Coat. Technol. 213 (2012) 126.
[33] Y. Situ, T. Huang, Y. Chen, W. Huang, H. Huang, Ceram. Int. 40 (2014) 919.
[34] C. Yang, W. Huang, T. Huang, H. Huang, Sci. Adv. Mater. 6 (2014) 9.
[35] H. Gao, J. Tian, H. Kong, P. Yang, W. Zhang, J. Chu, Surf. Coat. Technol. 228 (2013) 162.
[36] X. Li, P. Wu, H. Qiu, S. Chen, B. Song, Thin Solid Films 520 (2012) 2316.
[37] D. Turnbull, Solid State Phys. 3 (1956) 225.

[38] Y. Chen, W. Huang, D. He, Y. Situ, H. Huang, ACS Appl, Mater. Interfaces 6 (2014) 14405.
[39] X. Zhou, F. Peng, H. Wang, H. Yu, Y. Fang, Chem. Commun. 48 (2012) 600.
[40] C. Zhu, B. Lu, Q. Su, E. Xie, W. Lan, Nanoscale 4 (2012) 3060.
[41] A. Perez-Larios, R. Lopez, A. Hernandez-Gordillo, F. Tzompantzi, R. Gomez, L.M. Torres-Guerra, Fuel 100 (2012) 139.
[42] C. Chen, J. Liu, P. Liu, B. Yu, Adv. Chem. Eng. Sci. 1 (2011) 9.
[43] J. Tian, L. Chen, Y. Yin, X. Wang, J. Dai, Z. Zhu, X. Liu, P. Wu, Surf. Coat. Technol. 204 (2009) 205.
[44] V. Musat, A. Rego, R. Monteiro, E. Fortunato, Thin Solid Films 516 (2008) 1512.
[45] J. Yu, X. Zhao, J. Mater. Sci. Lett. 20 (2001) 671.
[46] R. Fateh, R. Dillert, D. Bahnemann, Langmuir 29 (2013) 3730.
[47] S. Liao, H. Donggen, D. Yu, Y. Su, G. Yuan, J. Photochem. Photobiol. A Chem. 168 (2004) 7.
[48] K. Tanabe, T. Sumiyoshi, K. Shibata, T. Kiyoura, J. Kitagawa, Bull. Chem. Soc. Jpn. 47 (1974) 1064.
[49] A. Mills, M. Crow, Int. J. Photoenergy 2008 (2008) 1.
[50] H. Irie, K. Hashimoto, Environmental Photochemistry Part II, Springer, 2005, pp. 425–450.
[51] B. Ohtani, Y. Ogawa, S.-i. Nishimoto, J. Phys. Chem. B 101 (1997) 3746.